

MIT Open Access Articles

*Observation of Two New Ξ [subscript b]
[superscript -] Baryon Resonances*

The MIT Faculty has made this article openly available. **Please share** how this access benefits you. Your story matters.

Citation: Aaij, R. et al. "Observation of Two New Ξ [subscript b][superscript -] Baryon Resonances." Physical Review Letters 114.6 (2015).

As Published: <http://dx.doi.org/10.1103/PhysRevLett.114.062004>

Publisher: American Physical Society

Persistent URL: <http://hdl.handle.net/1721.1/94493>

Version: Final published version: final published article, as it appeared in a journal, conference proceedings, or other formally published context

Terms of use: Creative Commons Attribution





Observation of Two New Ξ_b^- Baryon Resonances

R. Aaij *et al.**

(LHCb Collaboration)

(Received 18 November 2014; published 10 February 2015)

Two structures are observed close to the kinematic threshold in the $\Xi_b^0\pi^-$ mass spectrum in a sample of proton-proton collision data, corresponding to an integrated luminosity of 3.0 fb^{-1} , recorded by the LHCb experiment. In the quark model, two baryonic resonances with quark content bds are expected in this mass region: the spin-parity $J^P = (1/2)^+$ and $J^P = (3/2)^+$ states, denoted $\Xi_b^{\prime-}$ and Ξ_b^{*-} . Interpreting the structures as these resonances, we measure the mass differences and the width of the heavier state to be $m(\Xi_b^{\prime-}) - m(\Xi_b^0) - m(\pi^-) = 3.653 \pm 0.018 \pm 0.006 \text{ MeV}/c^2$, $m(\Xi_b^{*-}) - m(\Xi_b^0) - m(\pi^-) = 23.96 \pm 0.12 \pm 0.06 \text{ MeV}/c^2$, $\Gamma(\Xi_b^{*-}) = 1.65 \pm 0.31 \pm 0.10 \text{ MeV}$, where the first and second uncertainties are statistical and systematic, respectively. The width of the lighter state is consistent with zero, and we place an upper limit of $\Gamma(\Xi_b^{\prime-}) < 0.08 \text{ MeV}$ at 95% confidence level. Relative production rates of these states are also reported.

DOI: 10.1103/PhysRevLett.114.062004

PACS numbers: 14.20.Mr, 13.30.Eg

In the constituent quark model [1,2], baryonic states form multiplets according to the symmetry of their flavor, spin, and spatial wave functions. The Ξ_b states form isodoublets composed of a Ξ_b^0 ($b s u$) and a Ξ_b^- ($b s d$) state. Three such Ξ_b isodoublets that are neither orbitally nor radially excited are expected to exist, and can be categorized by the spin j of the su or sd diquark and the spin parity J^P of the baryon: one with $j = 0$ and $J^P = (1/2)^+$, one with $j = 1$ and $J^P = (1/2)^+$, and one with $j = 1$ and $J^P = (3/2)^+$. This follows the same pattern as the well-known Ξ_c states [3], and we, therefore, refer to these three isodoublets as the Ξ_b , the Ξ_b^{\prime} , and the Ξ_b^* . The spin-antisymmetric $J^P = (1/2)^+$ state, observed by multiple experiments [4–11], is the lightest and, therefore, decays through the weak interaction. The others should decay predominantly strongly through a P -wave pion transition ($\Xi_b^{(i,*)} \rightarrow \Xi_b \pi$) if their masses are above the kinematic threshold for such a decay; otherwise, they should decay electromagnetically ($\Xi_b^{(i,*)} \rightarrow \Xi_b \gamma$). Observing such electromagnetic decays at hadron colliders is challenging due to large photon multiplicities and worse energy resolution for low energy photons compared to charged particles.

There are numerous predictions for the mass spectrum of these low-lying states [12–23]. The consensus is that the isospin-averaged value of the mass difference $m(\Xi_b^*) - m(\Xi_b)$ is above threshold for strong decay but that the isospin-averaged difference $m(\Xi_b^{\prime}) - m(\Xi_b)$ is near the kinematic threshold. However, it is expected that the mass

difference $m(\Xi_b^{\prime-}) - m(\Xi_b^0)$ is larger than $m(\Xi_b^0) - m(\Xi_b^-)$ due to the relatively large isospin splitting between the charged and neutral Ξ_b states. For the ground state, the measured isospin splitting of $m(\Xi_b^-) - m(\Xi_b^0) = 5.92 \pm 0.64 \text{ MeV}/c^2$ [24] is in good agreement with the predicted value of $6.24 \pm 0.21 \text{ MeV}/c^2$ [13]. While the equivalent isospin splitting for the Ξ_b^{\prime} and Ξ_b^* states is likely to be smaller due to differences in the hyperfine mass corrections, the mass difference $m(\Xi_b^{\prime-}) - m(\Xi_b^0)$ could well be 5–10 MeV/c^2 larger than $m(\Xi_b^0) - m(\Xi_b^-)$. It is, therefore, plausible that the decay $\Xi_b^{\prime-} \rightarrow \Xi_b^0 \pi^-$ is kinematically allowed, while $\Xi_b^0 \rightarrow \Xi_b^- \pi^+$ is not. This is consistent with the recent CMS observation [25] of a single peak in the $\Xi_b^- \pi^+$ mass spectrum, interpreted as the Ξ_b^{*0} resonance. We note that $\Xi_b^0 \rightarrow \Xi_b^0 \pi^0$ may also be allowed even if $\Xi_b^0 \rightarrow \Xi_b^- \pi^+$ is not.

In this Letter, we present the results of a study of the $\Xi_b^0\pi^-$ mass spectrum using pp collision data recorded by the LHCb experiment, corresponding to an integrated luminosity of 3.0 fb^{-1} . One third of the data were collected at a center-of-mass energy of 7 TeV and the remainder at 8 TeV. We observe two highly significant structures, which are interpreted as the $\Xi_b^{\prime-}$ and Ξ_b^{*-} baryons. The properties of these new states are reported. Charge-conjugate processes are implicitly included.

The LHCb detector [26] is a single-arm forward spectrometer covering the pseudorapidity range $2 < \eta < 5$, designed for the study of particles containing b or c quarks. The detector includes a high-precision tracking system, which provides a momentum measurement with precision of about 0.5% from 2–100 GeV/c and impact parameter resolution of approximately 20 μm for particles with large transverse momentum (p_T). Ring-imaging Cherenkov detectors [27] are used to distinguish charged hadrons.

*Full author list given at the end of the article.

Published by the American Physical Society under the terms of the Creative Commons Attribution 3.0 License. Further distribution of this work must maintain attribution to the author(s) and the published articles title, journal citation, and DOI.

Photon, electron, and hadron candidates are identified using a calorimeter system, which is followed by detectors to identify muons [28].

The trigger [29] consists of a hardware stage, based on information from the calorimeter and muon systems, followed by a software stage. The software trigger requires a two-, three-, or four-track secondary vertex which is significantly displaced from all primary pp vertices (PVs) and for which the scalar p_T sum of the charged particles is large. At least one particle should have $p_T > 1.7$ GeV/ c and be inconsistent with coming from any of the PVs. A multivariate algorithm [30] is used to identify secondary vertices consistent with the decay of a b hadron.

In the simulation, pp collisions are generated using PYTHIA [31] with a specific LHCb configuration [32]. Decays of hadrons are described by EVTGEN [33], in which final-state radiation is generated using PHOTOS [34]. The interaction of the generated particles with the detector, and its response, are implemented using the GEANT4 toolkit [35] as described in Ref. [36].

Signal candidates are reconstructed in the final state $\Xi_b^0 \pi_s^-$, where $\Xi_b^0 \rightarrow \Xi_c^+ \pi^-$ and $\Xi_c^+ \rightarrow p K^- \pi^+$. The first pion is denoted π_s^- to distinguish it from the others. The Ξ_b^0 decay mode is the same as that studied in [9], and the selection used for this analysis is heavily inspired by it and by other LHCb studies with baryons or low-momentum pions in the final state (e.g., [37,38]). At each stage of the decay chain, the particles are required to meet at a common vertex with good fit quality. In the case of the $\Xi_b^0 \pi_s^-$ candidate, this vertex is constrained to be consistent with one of the PVs in the event. Track quality requirements are applied, along with momentum and transverse momentum requirements, to reduce combinatorial background. Particle identification criteria are applied to the final-state tracks to suppress background from misidentified particles. To remove cross feed from other charm hadrons, Ξ_c^+ candidates are rejected if they are consistent with $D^+ \rightarrow K^+ K^- \pi^+$, $D_s^+ \rightarrow K^+ K^- \pi^+$, $D^+ \rightarrow \pi^+ K^- \pi^+$, or $D^{*+} \rightarrow D^0(K^+ K^-) \pi^+$ decays. To reduce background formed from tracks originating at the PV, the decay vertices of Ξ_c^+ and Ξ_b^0 candidates are required to be significantly displaced from all PVs.

The Ξ_c^+ candidates are required to have an invariant mass within 20 MeV/ c^2 of the known mass [3], corresponding to approximately $\pm 3\sigma_{\Xi_c^+}$ where $\sigma_{\Xi_c^+}$ is the mass resolution. Candidate Ξ_b^0 decays are required to satisfy $5765 < m_{\text{cand}}(\Xi_b^0) - m_{\text{cand}}(\Xi_c^+) + m_{\Xi_c^+} < 5825$ MeV/ c^2 , where m_{cand} and $m_{\Xi_c^+}$ refer to the candidate and world-average masses, corresponding to approximately $\pm 2\sigma_{\Xi_b^0}$. In addition, the following kinematic requirements are imposed: $p_T(\Xi_c^+) > 1$ GeV/ c , $p_T(\Xi_b^0) > 2$ GeV/ c , $p_T(\Xi_b^0 \pi_s^-) > 2.5$ GeV/ c , and $p_T(\pi_s^-) > 0.15$ GeV/ c . Defining $\delta m \equiv m_{\text{cand}}(\Xi_b^0 \pi_s^-) - m_{\text{cand}}(\Xi_b^0) - m_{\pi^-}$, the region of consideration is $\delta m < 45$ MeV/ c^2 . There are,

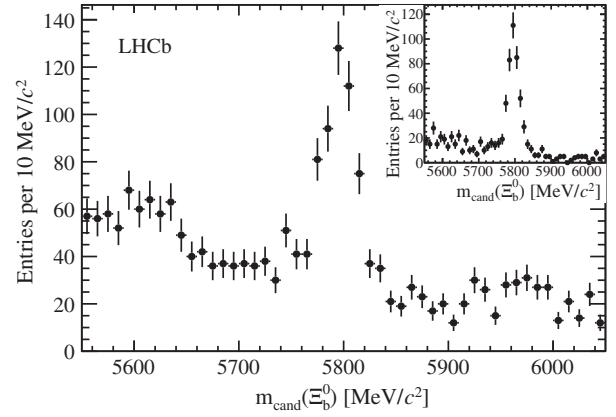


FIG. 1. Distribution of $m_{\text{cand}}(\Xi_b^0)$ for $\Xi_b^0 \pi_s^-$ candidates passing the full selection apart from the $m_{\text{cand}}(\Xi_b^0)$ requirement. Inset: The subset of candidates that lie in the δm signal regions of $3.0 < \delta m < 4.2$ MeV/ c^2 and $21 < \delta m < 27$ MeV/ c^2 .

on average, 1.15 candidates retained in this region per event. Such multiple candidates are due almost entirely to cases where the same Ξ_b^0 candidate is combined with different π_s^- candidates from the same PV. All $\Xi_b^0 \pi_s^-$ candidates are kept.

The $m_{\text{cand}}(\Xi_b^0)$ projection of the $\Xi_b^0 \pi_s^-$ candidates passing the full selection apart from the $m_{\text{cand}}(\Xi_b^0)$ requirement, but including the δm requirement, is shown in Fig. 1. Control samples, notably wrong-sign combinations $\Xi_b^0 \pi^+$, are also used to study backgrounds. The δm spectra for the signal and the wrong-sign sample are shown in Fig. 2. Two peaks are clearly visible, a narrow one at $\delta m \approx 3.7$ MeV/ c^2 and a broader one at $\delta m \approx 24$ MeV/ c^2 . No structure is observed in the wrong-sign sample, nor in studies of the Ξ_b^0 mass sidebands.

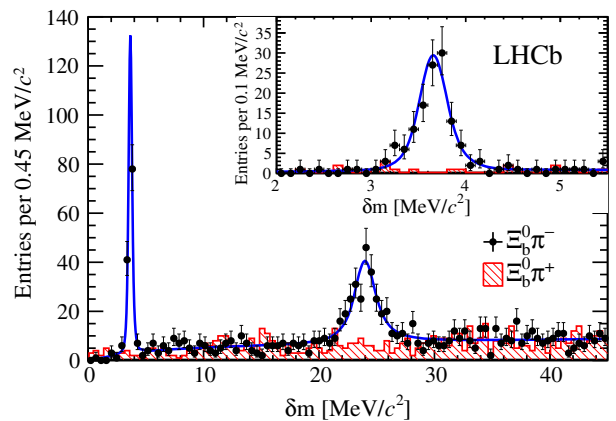


FIG. 2 (color online). Distribution of the mass difference, δm , for $\Xi_b^0 \pi_s^-$ candidates in data. The points with error bars show right-sign candidates in the Ξ_b^0 mass signal region, and the hatched histogram shows wrong-sign candidates with the same selection. The curve shows the nominal fit to the right-sign candidates. Inset: detail of the region 2.0–5.5 MeV/ c^2 .

Accurate determination of the masses, widths, and signal yields of these two states requires knowledge of the signal shapes, and in particular, the mass resolution of the two peaks. These are obtained from large samples of simulated decays with δm values of $3.69 \text{ MeV}/c^2$ and $23.69 \text{ MeV}/c^2$, corresponding to the two peaks. The natural widths, Γ , are set to negligible values so that the width measured in simulation is due entirely to the mass resolution. The resolution function is parametrized as the sum of three Gaussian distributions with independent mean values. Separate sets of parameters are determined for the two peaks. An indication of the scale of the resolution is given by the weighted averages of the three Gaussian widths, which are $0.21 \text{ MeV}/c^2$ and $0.54 \text{ MeV}/c^2$ for the lower- and higher-mass peaks. In the nominal fits to data, the parameters of the three Gaussian distributions are kept fixed to the values obtained from simulation, given in the Supplemental Material [39]. Small corrections, obtained from simulation, are applied to the masses to account for offsets in the resolution functions. The combinatorial background is modeled by a threshold function of the form

$$f(\delta m) = (1 - e^{-\delta m/C})(\delta m)^A,$$

where A and C are freely varying parameters determined in the fit to the data.

The masses, widths, and yields of the two peaks are determined from an unbinned maximum likelihood fit to the δm spectrum. In an initial fit, each peak is described using a P -wave relativistic Breit-Wigner (RBW) line shape [40] with a Blatt-Weisskopf barrier factor [41], convolved with the resolution function obtained from simulation. The fitted width of the lower-mass peak is found to be consistent with zero, and consequently, its width is set to zero in the nominal fit, shown in Fig. 2. The fitted yields in the lower- and higher-mass peaks are 121 ± 12 and 237 ± 24 events, with statistical significances in excess of 10σ . The nonzero value of the natural width of the higher-mass peak is also highly significant: the change in likelihood when the width is fixed to zero corresponds to a p value of 4×10^{-14} using Wilks's theorem [42].

An upper limit on the natural width of the lower-mass peak is set using ensembles of pseudoexperiments with the same parameters as in data, but with natural widths ranging from 0.01 to 0.12 MeV. The upper limit is taken to be the value of Γ for which a width equal to or greater than that obtained in data is observed in 95% of the pseudoexperiments. The resulting upper limit is $\Gamma(\Xi_b^{\prime-}) < 0.08 \text{ MeV}$ at 95% confidence level (C.L.).

A number of cross checks are performed to ensure the robustness of the measured masses and natural widths of these states and to assess systematic uncertainties. These include changing the assumed angular momentum (spin 0, 2) and radial parameter (1–5 GeV^{-1}) of the RBW and barrier factor, inflating the widths of the resolution

functions by a fixed factor of 1.1, the value found in a large $D^{*+} \rightarrow D^0\pi$ data sample [43], inflating the widths of the resolution functions by a common factor floated in the fit (with 1.03 ± 0.11 obtained), using a symmetric resolution function, using a nonrelativistic BW for the higher-mass peak, using a different background function, varying the fit range, checking the effect of finite sample size and of the variation of mass resolution with particle mass, keeping only one candidate in each event, imposing additional trigger requirements, separating the data by charge and LHCb magnet polarity, and fitting the wrong-sign sample. Where appropriate, systematic uncertainties are assigned based on the differences between the nominal results and those obtained in these tests. The calibration of the momentum scale [11,44] is validated by measuring $m(D^{*+}) - m(D^0)$ in a large sample of $D^{*+}, D^0 \rightarrow K^-K^+$ decays [43]. The mass difference agrees with a recent *BABAR* measurement [45] within $6 \text{ keV}/c^2$, corresponding to 1.3σ when including the mass scale uncertainty for that decay. The uncertainties are summarized in Table I. Taking these into account, we obtain

$$\delta m(\Xi_b^{\prime-}) = 3.653 \pm 0.018 \pm 0.006 \text{ MeV}/c^2,$$

$$\delta m(\Xi_b^{*-}) = 23.96 \pm 0.12 \pm 0.06 \text{ MeV}/c^2,$$

$$\Gamma(\Xi_b^{*-}) = 1.65 \pm 0.31 \pm 0.10 \text{ MeV},$$

$$\Gamma(\Xi_b^{\prime-}) < 0.08 \text{ MeV at } 95\% \text{ C.L.}$$

Combining these with the measurement of $m(\Xi_b^0) = 5791.80 \pm 0.50 \text{ MeV}/c^2$ obtained previously at LHCb [9], the masses of these states are found to be

$$m(\Xi_b^{\prime-}) = 5935.02 \pm 0.02 \pm 0.01 \pm 0.50 \text{ MeV}/c^2,$$

$$m(\Xi_b^{*-}) = 5955.33 \pm 0.12 \pm 0.06 \pm 0.50 \text{ MeV}/c^2,$$

where the uncertainties are statistical, systematic, and due to the $m(\Xi_b^0)$ measurement, respectively.

Helicity angle [46] distributions may be used to distinguish between spin hypotheses for resonances. We consider the decay sequence $\Xi_b^{(\prime,*)-} \rightarrow \Xi_b^0\pi^-, \Xi_b^0 \rightarrow \Xi_c^+\pi^-$,

TABLE I. Systematic uncertainties, in units of MeV/c^2 (masses) and MeV (width). The statistical uncertainties are also shown for comparison.

Source	$\delta m(\Xi_b^{\prime-})$	$\delta m(\Xi_b^{*-})$	$\Gamma(\Xi_b^{*-})$
Simulated sample size	0.002	0.005	
Multiple candidates	0.004	0.048	0.055
Resolution model	0.002	0.003	0.070
Background description	0.001	0.003	0.019
Momentum scale	0.003	0.014	0.003
RBW spin and radial parameter	0.000	0.023	0.028
Sum in quadrature	0.006	0.055	0.095
Statistical uncertainty	0.018	0.119	0.311

where the $\Xi_b^{(\prime,*)-}$ has spin J and the Ξ_b^0 , Ξ_c^+ , and π^- have spin-parity $(1/2)^+$, $(1/2)^+$, and 0^- , respectively, which is analogous to the scenario considered in Ref. [47]. Defining θ_h as the angle between the three-momentum of the Ξ_b^0 in the $\Xi_b^{(\prime,*)-}$ rest frame and the three-momentum of the Ξ_c^+ in the Ξ_b^0 rest frame, the $\cos\theta_h$ distribution is a polynomial of order $(2J-1)$. For $J = \frac{1}{2}$, this would yield a flat distribution, and hence, a nonuniform distribution would imply $J > \frac{1}{2}$. The converse does not follow, however: a higher-spin resonance that is unpolarized will lead to a flat distribution. For each of the two peaks, the background-subtracted, efficiency-corrected $\cos\theta_h$ distributions are studied. Both are found to be consistent with flat distributions. When fitted with a function of the form $f(\cos\theta_h) = [a + 3(1-a)\cos^2\theta_h]/2$, the fitted values of a are 0.89 ± 0.11 and 0.88 ± 0.11 , and the quality of the fits does not improve significantly. Thus, the available data are consistent with the quark model expectations that the lower-mass peak corresponds to a $J = \frac{1}{2}$ state and the higher one to a $J = \frac{3}{2}$ state (if unpolarized or weakly polarized), but other values of J are not excluded.

We measure the production rates of the two signals relative to that of the Ξ_b^0 state, selected inclusively and passing the same Ξ_b^0 selection criteria as the signal sample. To remain within the bandwidth restrictions of the off-line data reduction process, 10% of the candidates in the normalization mode are randomly selected and retained for use in this analysis. To ensure that the efficiencies are well understood, we use only the subset of events in which one or more of the Ξ_b^0 decay products is consistent with activating the hardware trigger in the calorimeter.

For this subsample of events, the fitted yields are 93 ± 10 for the lower-mass $\Xi_b^0\pi_s^-$ state, 166 ± 20 for the higher-mass $\Xi_b^0\pi_s^-$ state, and 162 ± 15 for the Ξ_b^0 normalization sample. The efficiency ratios are determined with simulated decays, applying the same trigger, reconstruction, and selection procedures that are used for the data. Systematic uncertainties (and, where appropriate, corrections) are assigned for those sources that do not cancel in the efficiency ratios. These uncertainties include the modeling of the Ξ_b momentum spectra, the π_s^- reconstruction efficiency [48], the fit method, and the efficiency of those selection criteria that are applied to the $\Xi_b^0\pi_s^-$ candidates but not to the Ξ_b^0 normalization mode. Combining the 7 and 8 TeV data samples, the results obtained are

$$\frac{\sigma(pp \rightarrow \Xi_b^{\prime-} X) \mathcal{B}(\Xi_b^{\prime-} \rightarrow \Xi_b^0 \pi^-)}{\sigma(pp \rightarrow \Xi_b^0 X)} = 0.118 \pm 0.017 \pm 0.007,$$

$$\frac{\sigma(pp \rightarrow \Xi_b^{*-} X) \mathcal{B}(\Xi_b^{*-} \rightarrow \Xi_b^0 \pi^-)}{\sigma(pp \rightarrow \Xi_b^0 X)} = 0.207 \pm 0.032 \pm 0.015,$$

$$\frac{\sigma(pp \rightarrow \Xi_b^{*-} X) \mathcal{B}(\Xi_b^{*-} \rightarrow \Xi_b^0 \pi^-)}{\sigma(pp \rightarrow \Xi_b^{\prime-} X) \mathcal{B}(\Xi_b^{\prime-} \rightarrow \Xi_b^0 \pi^-)} = 1.74 \pm 0.30 \pm 0.12,$$

where the first and second uncertainties are statistical and systematic, respectively, σ denotes a cross section measured within the LHCb acceptance and extrapolated to the full kinematic range with PYTHIA, \mathcal{B} represents a branching fraction, and X refers to the rest of the event. Given that isospin partner modes $\Xi_b^0 \rightarrow \Xi_b^0 \pi^0$ and $\Xi_b^{*0} \rightarrow \Xi_b^0 \pi^0$ are also expected, these results imply that a large fraction of Ξ_b^0 baryons in the forward region are produced in the decays of Ξ_b resonances.

As a further check, the $\Xi_b^0\pi_s^-$ mass spectrum is studied with additional Ξ_b^0 decay modes. Significant peaks are seen with the mode $\Xi_b^0 \rightarrow \Lambda_c^+(pK^-\pi^+)K^-\pi^+\pi^-$ for both $\Xi_b^{\prime-}$ (6.4σ) and Ξ_b^{*-} (4.7σ). The peaks are also seen with reduced significance in other Ξ_b^0 final states: 4σ for $\Xi_b^{\prime-}$ and 2σ for Ξ_b^{*-} in $\Xi_b^0 \rightarrow D^0(K^-\pi^+)pK^-$, and 3σ for $\Xi_b^{\prime-}$ and 3σ for Ξ_b^{*-} in $\Xi_b^0 \rightarrow D^+(K^-\pi^+\pi^+)pK^-\pi^-$. The modes $\Xi_b^0 \rightarrow \Lambda_c^+(pK^-\pi^+)K^-\pi^+\pi^-$ and $\Xi_b^0 \rightarrow D^+(K^-\pi^+\pi^+)pK^-\pi^-$ have not been observed before, and are being studied in separate analyses.

With a specific configuration of other excited Ξ_b states, it is possible to produce a narrow peak in the $\Xi_b^0\pi^-$ mass spectrum that is not due to a $\Xi_b^{\prime-}$ resonance. This can arise from the decay chain $\Xi_b^{*-} \rightarrow \Xi_b^0\pi^-$, $\Xi_b^0 \rightarrow \Xi_b^0\pi^0$, where the Ξ_b^{*-} is the $L=1$, $J^P = (1/2)^-$ state analogous to the $\Xi_c(2790)$. If both decays are close to threshold, the particles produced will be kinematically correlated such that combining the Ξ_b^0 daughter with the π^- from the Ξ_b^{*-} would produce a structure in the $m(\Xi_b^0\pi^-)$ spectrum. In general, such a structure would be broader than that seen in Fig. 2 and would be accompanied by a similar peak in the wrong-sign $\Xi_b^0\pi^+$ spectrum from the isospin-partner decay, $\Xi_b^{*0} \rightarrow \Xi_b^{\prime-}\pi^+$, $\Xi_b^{\prime-} \rightarrow \Xi_b^0\pi^-$. However, if a number of conditions are fulfilled, including the Ξ_b^{*-} and Ξ_b^0 states being 279.0 ± 0.5 and 135.8 ± 0.5 MeV/ c^2 heavier than the Ξ_b^0 ground state, respectively, it is possible to circumvent these constraints. This would also require that the production rate of the $L=1$ state be comparable to that of the $L=0$, $J^P = (3/2)^+$ state. Although this scenario is contrived, it cannot be excluded at present.

In conclusion, two structures are observed with high significance in the $\Xi_b^0\pi^-$ mass spectrum with mass differences above threshold of $\delta m = 3.653 \pm 0.018 \pm 0.006$ MeV/ c^2 and $23.96 \pm 0.12 \pm 0.06$ MeV/ c^2 . These values are in general agreement with quark model expectations for the $J^P = (1/2)^+$ $\Xi_b^{\prime-}$ and $J^P = (3/2)^+$ Ξ_b^{*-} states. Their natural widths are measured to be $\Gamma(\Xi_b^{\prime-}) < 0.08$ MeV at 95% C.L. and $\Gamma(\Xi_b^{*-}) = 1.65 \pm 0.31 \pm 0.10$ MeV. The observed angular distributions in the decays of these states are consistent with the spins expected in the quark model, but other J values are not excluded. The relative production rates are also measured.

We express our gratitude to our colleagues in the CERN accelerator departments for the excellent performance of

the LHC. We thank the technical and administrative staff at the LHCb institutes. We acknowledge support from CERN and from the national agencies: CAPES, CNPq, FAPERJ, and FINEP (Brazil); NSFC (China); CNRS/IN2P3 (France); BMBF, DFG, HGF, and MPG (Germany); INFN (Italy); FOM and NWO (Netherlands); MNiSW and NCN (Poland); MEN/IFA (Romania); MinES and FANO (Russia); MinECo (Spain); SNSF and SER (Switzerland); NASU (Ukraine); STFC (United Kingdom); NSF (USA). The Tier1 computing centres are supported by IN2P3 (France), KIT and BMBF (Germany), INFN (Italy), NWO and SURF (Netherlands), PIC (Spain), GridPP (United Kingdom). We are indebted to the communities behind the multiple open source software packages on which we depend. We are also thankful for the computing resources and the access to software R&D tools provided by Yandex LLC (Russia). Individual groups or members have received support from EPLANET, Marie Skłodowska-Curie Actions and ERC (European Union), Conseil général de Haute-Savoie, Labex ENIGMASS and OCEVU, Région Auvergne (France), RFBR (Russia), XuntaGal and GENCAT (Spain), Royal Society and Royal Commission for the Exhibition of 1851 (United Kingdom).

-
- [1] M. Gell-Mann, *Phys. Lett.* **8**, 214 (1964).
 [2] G. Zweig, Developments in the Quark Theory of Hadrons **1**, 22 (1980).
 [3] K. A. Olive *et al.* (Particle Data Group), *Chin. Phys. C* **38**, 090001 (2014).
 [4] T. Aaltonen *et al.* (CDF Collaboration), *Phys. Rev. Lett.* **99**, 052002 (2007).
 [5] V. Abazov *et al.* (D0 Collaboration), *Phys. Rev. Lett.* **99**, 052001 (2007).
 [6] T. Aaltonen *et al.* (CDF Collaboration), *Phys. Rev. D* **80**, 072003 (2009).
 [7] T. Aaltonen *et al.* (CDF Collaboration), *Phys. Rev. Lett.* **107**, 102001 (2011).
 [8] R. Aaij *et al.* (LHCb Collaboration), *Phys. Rev. D* **89**, 032001 (2014).
 [9] R. Aaij *et al.* (LHCb Collaboration), *Phys. Rev. Lett.* **113**, 032001 (2014).
 [10] T. Aaltonen *et al.* (CDF Collaboration), *Phys. Rev. D* **89**, 072014 (2014).
 [11] R. Aaij *et al.* (LHCb Collaboration), *Phys. Rev. Lett.* **110**, 182001 (2013).
 [12] E. Klempt and J.-M. Richard, *Rev. Mod. Phys.* **82**, 1095 (2010).
 [13] M. Karliner, B. Keren-Zur, H. J. Lipkin, and J. L. Rosner, *Ann. Phys. (Amsterdam)* **324**, 2 (2009).
 [14] R. Lewis and R. M. Woloshyn, *Phys. Rev. D* **79**, 014502 (2009).
 [15] D. Ebert, R. N. Faustov, and V. O. Galkin, *Phys. Rev. D* **72**, 034026 (2005).
 [16] X. Liu, H.-X. Chen, Y.-R. Liu, A. Hosaka, and S.-L. Zhu, *Phys. Rev. D* **77**, 014031 (2008).
 [17] E. E. Jenkins, *Phys. Rev. D* **77**, 034012 (2008).
 [18] M. Karliner, *Nucl. Phys. B, Proc. Suppl.* **187**, 21 (2009).
 [19] J.-R. Zhang and M.-Q. Huang, *Phys. Rev. D* **78**, 094015 (2008).
 [20] Z.-G. Wang, *Eur. Phys. J. C* **68**, 459 (2010).
 [21] Z. S. Brown, W. Detmold, S. Meinel, and K. Orginos, *Phys. Rev. D* **90**, 094507 (2014).
 [22] A. Valcarce, H. Garcilazo, and J. Vijande, *Eur. Phys. J. A* **37**, 217 (2008).
 [23] A. Limphirat, C. Kobdaj, P. Suebka, and Y. Yan, *Phys. Rev. C* **82**, 055201 (2010).
 [24] R. Aaij *et al.* (LHCb Collaboration), *Phys. Rev. Lett.* **113**, 242002 (2014).
 [25] S. Chatrchyan *et al.* (CMS Collaboration), *Phys. Rev. Lett.* **108**, 252002 (2012).
 [26] A. A. Alves Jr. *et al.* (LHCb Collaboration), *JINST* **3**, S08005 (2008).
 [27] M. Adinolfi *et al.*, *Eur. Phys. J. C* **73**, 2431 (2013).
 [28] A. A. Alves Jr. *et al.*, *JINST* **8**, P02022 (2013).
 [29] R. Aaij *et al.*, *JINST* **8**, P04022 (2013).
 [30] V. V. Gligorov and M. Williams, *JINST* **8**, P02013 (2013).
 [31] T. Sjöstrand, S. Mrenna, and P. Skands, *J. High Energy Phys.* **05** (2006) 026; *Comput. Phys. Commun.* **178**, 852 (2008).
 [32] I. Belyaev *et al.*, in *Nuclear Science Symposium Conference Record (NSS/MIC)* (IEEE, New York, 2010), p. 1155.
 [33] D. J. Lange, *Nucl. Instrum. Methods Phys. Res., Sect. A* **462**, 152 (2001).
 [34] P. Golonka and Z. Was, *Eur. Phys. J. C* **45**, 97 (2006).
 [35] J. Allison, K. Amako, J. Apostolakis, H. Araujo, P. Dubois *et al.* (GEANT4 Collaboration), *IEEE Trans. Nucl. Sci.* **53**, 270 (2006); S. Agostinelli *et al.* (GEANT4 Collaboration), *Nucl. Instrum. Methods Phys. Res., Sect. A* **506**, 250 (2003).
 [36] M. Clemencic, G. Corti, S. Easo, C. R. Jones, S. Miglioranza, M. Pappagallo, and P. Robbe, *J. Phys. Conf. Ser.* **331**, 032023 (2011).
 [37] R. Aaij *et al.* (LHCb Collaboration), *Phys. Rev. Lett.* **108**, 111602 (2012).
 [38] R. Aaij *et al.* (LHCb Collaboration), *J. High Energy Phys.* **12** (2013) 090.
 [39] See Supplemental Material at <http://link.aps.org/supplemental/10.1103/PhysRevLett.114.062004> for further discussion of the possible feed down, helicity angle distributions, and the resolution functions used.
 [40] J. D. Jackson, *Nuovo Cimento* **34**, 1644 (1964).
 [41] J. Blatt and V. Weisskopf, *Theoretical Nuclear Physics* (John Wiley & Sons, New York, 1952).
 [42] S. Wilks, *Ann. Math. Stat.* **9**, 60 (1938).
 [43] R. Aaij *et al.* (LHCb Collaboration), Report No. LHCb-CONF-2013-003.
 [44] R. Aaij *et al.* (LHCb Collaboration), *J. High Energy Phys.* **06** (2013) 065.
 [45] J. P. Lees *et al.* (BABAR Collaboration), *Phys. Rev. D* **88**, 052003 (2013); *Phys. Rev. Lett.* **111**, 111801 (2013).
 [46] J. D. Richman, Report No. CALT-68-1148.
 [47] R. Mizuk *et al.*, *Phys. Rev. Lett.* **98**, 262001 (2007).
 [48] R. Aaij *et al.* (LHCb Collaboration), arXiv:1408.1251.

R. Aaij,⁴¹ B. Adeva,³⁷ M. Adinolfi,⁴⁶ A. Affolder,⁵² Z. Ajaltouni,⁵ S. Akar,⁶ J. Albrecht,⁹ F. Alessio,³⁸ M. Alexander,⁵¹ S. Ali,⁴¹ G. Alkhazov,³⁰ P. Alvarez Cartelle,³⁷ A. A. Alves Jr,^{25,38} S. Amato,² S. Amerio,²² Y. Amhis,⁷ L. An,³ L. Anderlini,^{17,a} J. Anderson,⁴⁰ R. Andreassen,⁵⁷ M. Andreotti,^{16,b} J. E. Andrews,⁵⁸ R. B. Appleby,⁵⁴ O. Aquines Gutierrez,¹⁰ F. Archilli,³⁸ A. Artamonov,³⁵ M. Artuso,⁵⁹ E. Aslanides,⁶ G. Auriemma,^{25,c} M. Baalouch,⁵ S. Bachmann,¹¹ J. J. Back,⁴⁸ A. Badalov,³⁶ C. Baesso,⁶⁰ W. Baldini,¹⁶ R. J. Barlow,⁵⁴ C. Barschel,³⁸ S. Barsuk,⁷ W. Barter,⁴⁷ V. Batozskaya,²⁸ V. Battista,³⁹ A. Bay,³⁹ L. Beaucourt,⁴ J. Beddow,⁵¹ F. Bedeschi,²³ I. Bediaga,¹ S. Belogurov,³¹ K. Belous,³⁵ I. Belyaev,³¹ E. Ben-Haim,⁸ G. Bencivenni,¹⁸ S. Benson,³⁸ J. Benton,⁴⁶ A. Berezhnov,³² R. Bernet,⁴⁰ A. Bertolin,²² M.-O. Bettler,⁴⁷ M. van Beuzekom,⁴¹ A. Bien,¹¹ S. Bifani,⁴⁵ T. Bird,⁵⁴ A. Bizzeti,^{17,d} P. M. Bjørnstad,⁵⁴ T. Blake,⁴⁸ F. Blanc,³⁹ J. Blouw,¹⁰ S. Blusk,⁵⁹ V. Bocci,²⁵ A. Bondar,³⁴ N. Bondar,^{30,38} W. Bonivento,¹⁵ S. Borghi,⁵⁴ A. Borgia,⁵⁹ M. Borsato,⁷ T. J. V. Bowcock,⁵² E. Bowen,⁴⁰ C. Bozzi,¹⁶ D. Brett,⁵⁴ M. Britsch,¹⁰ T. Britton,⁵⁹ J. Brodzicka,⁵⁴ N. H. Brook,⁴⁶ A. Bursche,⁴⁰ J. Buytaert,³⁸ S. Cadeddu,¹⁵ R. Calabrese,^{16,b} M. Calvi,^{20,e} M. Calvo Gomez,^{36,f} P. Campana,¹⁸ D. Campora Perez,³⁸ L. Capriotti,⁵⁴ A. Carbone,^{14,g} G. Carboni,^{24,h} R. Cardinale,^{19,38,i} A. Cardini,¹⁵ L. Carson,⁵⁰ K. Carvalho Akiba,^{2,38} RCM Casanova Mohr,³⁶ G. Casse,⁵² L. Cassina,^{20,e} L. Castillo Garcia,³⁸ M. Cattaneo,³⁸ Ch. Cauet,⁹ R. Cenci,^{23,j} M. Charles,⁸ Ph. Charpentier,³⁸ M. Chefdeville,⁴ S. Chen,⁵⁴ S.-F. Cheung,⁵⁵ N. Chiapolini,⁴⁰ M. Chrzaszcz,^{40,26} X. Cid Vidal,³⁸ G. Ciezarek,⁴¹ P. E. L. Clarke,⁵⁰ M. Clemencic,³⁸ H. V. Cliff,⁴⁷ J. Closier,³⁸ V. Coco,³⁸ J. Cogan,⁶ E. Cogneras,⁵ V. Cogoni,¹⁵ L. Cojocariu,²⁹ G. Collazuol,²² P. Collins,³⁸ A. Comerma-Montells,¹¹ A. Contu,^{15,38} A. Cook,⁴⁶ M. Coombes,⁴⁶ S. Coquereau,⁸ G. Corti,³⁸ M. Corvo,^{16,b} I. Counts,⁵⁶ B. Couturier,³⁸ G. A. Cowan,⁵⁰ D. C. Craik,⁴⁸ A. C. Crocombe,⁴⁸ M. Cruz Torres,⁶⁰ S. Cunliffe,⁵³ R. Currie,⁵³ C. D'Ambrosio,³⁸ J. Dalseno,⁴⁶ P. David,⁸ P. N. Y. David,⁴¹ A. Davis,⁵⁷ K. De Bruyn,⁴¹ S. De Capua,⁵⁴ M. De Cian,¹¹ J. M. De Miranda,¹ L. De Paula,² W. De Silva,⁵⁷ P. De Simone,¹⁸ C.-T. Dean,⁵¹ D. Decamp,⁴ M. Deckenhoff,⁹ L. Del Buono,⁸ N. Déléage,⁴ D. Derkach,⁵⁵ O. Deschamps,⁵ F. Dettori,³⁸ B. Dey,⁴⁰ A. Di Canto,³⁸ A. Di Domenico,²⁵ H. Dijkstra,³⁸ S. Donleavy,⁵² F. Dordei,¹¹ M. Dorigo,³⁹ A. Dosil Suárez,³⁷ D. Dossett,⁴⁸ A. Dovbnya,⁴³ K. Dreimanis,⁵² G. Dujany,⁵⁴ F. Dupertuis,³⁹ P. Durante,³⁸ R. Dzhelyadin,³⁵ A. Dziurda,²⁶ A. Dzyuba,³⁰ S. Easo,^{49,38} U. Egede,⁵³ V. Egorychev,³¹ S. Eidelman,³⁴ S. Eisenhardt,⁵⁰ U. Eitschberger,⁹ R. Ekelhof,⁹ L. Eklund,⁵¹ I. El Rifai,⁵ Ch. Elsasser,⁴⁰ S. Ely,⁵⁹ S. Esen,¹¹ H.-M. Evans,⁴⁷ T. Evans,⁵⁵ A. Falabella,¹⁴ C. Färber,¹¹ C. Farinelli,⁴¹ N. Farley,⁴⁵ S. Farry,⁵² R. Fay,⁵² D. Ferguson,⁵⁰ V. Fernandez Albor,³⁷ F. Ferreira Rodrigues,¹ M. Ferro-Luzzi,³⁸ S. Filippov,³³ M. Fiore,^{16,b} M. Fiorini,^{16,b} M. Firlej,²⁷ C. Fitzpatrick,³⁹ T. Fiutowski,²⁷ P. Fol,⁵³ M. Fontana,¹⁰ F. Fontanelli,^{19,i} R. Forty,³⁸ O. Francisco,² M. Frank,³⁸ C. Frei,³⁸ M. Frosini,¹⁷ J. Fu,^{21,38} E. Furfaro,^{24,h} A. Gallas Torreira,³⁷ D. Galli,^{14,g} S. Gallorini,^{22,38} S. Gambetta,^{19,i} M. Gandelman,² P. Gandini,⁵⁹ Y. Gao,³ J. García Pardiñas,³⁷ J. Garofoli,⁵⁹ J. Garra Tico,⁴⁷ L. Garrido,³⁶ D. Gascon,³⁶ C. Gaspar,³⁸ U. Gastaldi,¹⁶ R. Gauld,⁵⁵ L. Gavardi,⁹ G. Gazzoni,⁵ A. Geraci,^{21,k} E. Gersabeck,¹¹ M. Gersabeck,⁵⁴ T. Gershon,⁴⁸ Ph. Ghez,⁴ A. Gianelle,²² S. Giani,³⁹ V. Gibson,⁴⁷ L. Giubega,²⁹ V. V. Gligorov,³⁸ C. Göbel,⁶⁰ D. Golubkov,³¹ A. Golutvin,^{53,31,38} A. Gomes,^{1,l} C. Gotti,^{20,e} M. Grabalosa Gándara,⁵ R. Graciani Diaz,³⁶ L. A. Granado Cardoso,³⁸ E. Graugés,³⁶ E. Graverini,⁴⁰ G. Graziani,¹⁷ A. Grecu,²⁹ E. Greening,⁵⁵ S. Gregson,⁴⁷ P. Griffith,⁴⁵ L. Grillo,¹¹ O. Grünberg,⁶³ B. Gui,⁵⁹ E. Gushchin,³³ Yu. Guz,^{35,38} T. Gys,³⁸ C. Hadjivasiliou,⁵⁹ G. Haefeli,³⁹ C. Haen,³⁸ S. C. Haines,⁴⁷ S. Hall,⁵³ B. Hamilton,⁵⁸ T. Hampson,⁴⁶ X. Han,¹¹ S. Hansmann-Menzemer,¹¹ N. Harnew,⁵⁵ S. T. Harnew,⁴⁶ J. Harrison,⁵⁴ J. He,³⁸ T. Head,³⁹ V. Heijne,⁴¹ K. Hennessy,⁵² P. Henrard,⁵ L. Henry,⁸ J. A. Hernando Morata,³⁷ E. van Herwijnen,³⁸ M. Heß,⁶³ A. Hicheur,² D. Hill,⁵⁵ M. Hoballah,⁵ C. Hombach,⁵⁴ W. Hulsbergen,⁴¹ N. Hussain,⁵⁵ D. Hutchcroft,⁵² D. Hynds,⁵¹ M. Idzik,²⁷ P. Ilten,⁵⁶ R. Jacobsson,³⁸ A. Jaeger,¹¹ J. Jalocha,⁵⁵ E. Jans,⁴¹ P. Jaton,³⁹ A. Jawahery,⁵⁸ F. Jing,³ M. John,⁵⁵ D. Johnson,³⁸ C. R. Jones,⁴⁷ C. Joram,⁴⁵ B. Jost,³⁸ N. Jurik,⁵⁹ S. Kandybei,⁴³ W. Kanso,⁶ M. Karacson,³⁸ T. M. Karbach,³⁸ S. Karodia,⁵¹ M. Kelsey,⁵⁹ I. R. Kenyon,⁴⁵ T. Ketel,⁴² B. Khanji,^{20,38,e} C. Khurewathanakul,³⁹ S. Klaver,⁵⁴ K. Klimaszewski,²⁸ O. Kochebina,⁷ M. Kolpin,¹¹ I. Komarov,³⁹ R. F. Koopman,⁴² P. Koppenburg,^{41,38} M. Korolev,³² L. Kravchuk,³³ K. Kreplin,¹¹ M. Kreps,⁴⁸ G. Krocker,¹¹ P. Krokovny,³⁴ F. Kruse,⁹ W. Kucewicz,^{26,m} M. Kucharczyk,^{20,26,e} V. Kudryavtsev,³⁴ K. Kurek,²⁸ T. Kvaratskheliya,³¹ V. N. La Thi,³⁹ D. Lacarrere,³⁸ G. Lafferty,⁵⁴ A. Lai,¹⁵ D. Lambert,⁵⁰ R. W. Lambert,⁴² G. Lanfranchi,¹⁸ C. Langenbruch,⁴⁸ B. Langhans,³⁸ T. Latham,⁴⁸ C. Lazzeroni,⁴⁵ R. Le Gac,⁶ J. van Leerdam,⁴¹ J.-P. Lees,⁴ R. Lefèvre,⁵ A. Leflat,³² J. Lefrançois,⁷ O. Leroy,⁶ T. Lesiak,²⁶ B. Leverington,¹¹ Y. Li,³ T. Likhomanenko,⁶⁴ M. Liles,⁵² R. Lindner,³⁸ C. Linn,³⁸ F. Lionetto,⁴⁰ B. Liu,¹⁵ S. Lohn,³⁸ I. Longstaff,⁵¹ J. H. Lopes,² P. Lowdon,⁴⁰ D. Lucchesi,^{22,n} H. Luo,⁵⁰ A. Lupato,²² E. Luppi,^{16,b} O. Lupton,⁵⁵ F. Machefert,⁷ I. V. Machikhiliyan,³¹ F. Maciuc,²⁹ O. Maev,³⁰ S. Malde,⁵⁵ A. Malinin,⁶⁴

G. Manca,^{15,o} G. Mancinelli,⁶ A. Mapelli,³⁸ J. Maratas,⁵ J. F. Marchand,⁴ U. Marconi,¹⁴ C. Marin Benito,³⁶ P. Marino,^{23,j} R. Märki,³⁹ J. Marks,¹¹ G. Martellotti,²⁵ M. Martinelli,³⁹ D. Martinez Santos,⁴² F. Martinez Vidal,⁶⁵ D. Martins Tostes,² A. Massafferri,¹ R. Matev,³⁸ Z. Mathe,³⁸ C. Matteuzzi,²⁰ A. Mazurov,⁴⁵ M. McCann,⁵³ J. McCarthy,⁴⁵ A. McNab,⁵⁴ R. McNulty,¹² B. McSkelly,⁵² B. Meadows,⁵⁷ F. Meier,⁹ M. Meissner,¹¹ M. Merk,⁴¹ D. A. Milanes,⁶² M.-N. Minard,⁴ N. Moggi,¹⁴ J. Molina Rodriguez,⁶⁰ S. Monteil,⁵ M. Morandin,²² P. Morawski,²⁷ A. Mordà,⁶ M. J. Morello,^{23,j} J. Moron,²⁷ A.-B. Morris,⁵⁰ R. Mountain,⁵⁹ F. Muheim,⁵⁰ K. Müller,⁴⁰ M. Mussini,¹⁴ B. Muster,³⁹ P. Naik,⁴⁶ T. Nakada,³⁹ R. Nandakumar,⁴⁹ I. Nasteva,² M. Needham,⁵⁰ N. Neri,²¹ S. Neubert,³⁸ N. Neufeld,³⁸ M. Neuner,¹¹ A. D. Nguyen,³⁹ T. D. Nguyen,³⁹ C. Nguyen-Mau,^{39,p} M. Nicol,⁷ V. Niess,⁵ R. Niet,⁹ N. Nikitin,³² T. Nikodem,¹¹ A. Novoselov,³⁵ D. P. O'Hanlon,⁴⁸ A. Oblakowska-Mucha,²⁷ V. Obraztsov,³⁵ S. Ogilvy,⁵¹ O. Okhrimenko,⁴⁴ R. Oldeman,^{15,o} C. J. G. Onderwater,⁶⁶ M. Orlandea,²⁹ J. M. Otalora Goicochea,² A. Otto,³⁸ P. Owen,⁵³ A. Oyanguren,⁶⁵ B. K. Pal,⁵⁹ A. Palano,^{13,q} F. Palombo,^{21,r} M. Palutan,¹⁸ J. Panman,³⁸ A. Papanestis,^{49,38} M. Pappagallo,⁵¹ L. L. Pappalardo,^{16,b} C. Parkes,⁵⁴ C. J. Parkinson,^{9,45} G. Passaleva,¹⁷ G. D. Patel,⁵² M. Patel,⁵³ C. Patrignani,^{19,i} A. Pearce,^{54,49} A. Pellegrino,⁴¹ G. Penso,^{25,s} M. Pepe Altarelli,³⁸ S. Perazzini,^{14,g} P. Perret,⁵ L. Pescatore,⁴⁵ E. Pesen,⁶⁷ K. Petridis,⁵³ A. Petrolini,^{19,i} E. Picatoste Olloqui,³⁶ B. Pietrzyk,⁴ T. Pilař,⁴⁸ D. Pinci,²⁵ A. Pistone,¹⁹ S. Playfer,⁵⁰ M. Plo Casasus,³⁷ F. Polci,⁸ A. Poluektov,^{48,34} I. Polyakov,³¹ E. Polcarpo,² A. Popov,³⁵ D. Popov,¹⁰ B. Popovici,²⁹ C. Potterat,² E. Price,⁴⁶ J. D. Price,⁵² J. Prisciandaro,³⁹ A. Pritchard,⁵² C. Prouve,⁴⁶ V. Pugatch,⁴⁴ A. Puig Navarro,³⁹ G. Punzi,^{23,t} W. Qian,⁴ B. Rachwal,²⁶ J. H. Rademacker,⁴⁶ B. Rakotomiarmanana,³⁹ M. Rama,²³ M. S. Rangel,² I. Raniuk,⁴³ N. Rauschmayr,³⁸ G. Raven,⁴² F. Redi,⁵³ S. Reichert,⁵⁴ M. M. Reid,⁴⁸ A. C. dos Reis,¹ S. Ricciardi,⁴⁹ S. Richards,⁴⁶ M. Rihl,³⁸ K. Rinnert,⁵² V. Rives Molina,³⁶ P. Robbe,⁷ A. B. Rodrigues,¹ E. Rodrigues,⁵⁴ P. Rodriguez Perez,⁵⁴ S. Roiser,³⁸ V. Romanovsky,³⁵ A. Romero Vidal,³⁷ M. Rotondo,²² J. Rouvinet,³⁹ T. Ruf,³⁸ H. Ruiz,³⁶ P. Ruiz Valls,⁶⁵ J. J. Saborido Silva,³⁷ N. Sagidova,³⁰ P. Sail,⁵¹ B. Saitta,^{15,o} V. Salustino Guimaraes,² C. Sanchez Mayordomo,⁶⁵ B. Sanmartin Sedes,³⁷ R. Santacesaria,²⁵ C. Santamarina Rios,³⁷ E. Santovetti,^{24,h} A. Sarti,^{18,s} C. Satriano,^{25,c} A. Satta,²⁴ D. M. Saunders,⁴⁶ D. Savrina,^{31,32} M. Schiller,³⁸ H. Schindler,³⁸ M. Schlupp,⁹ M. Schmelling,¹⁰ B. Schmidt,³⁸ O. Schneider,³⁹ A. Schopper,³⁸ M.-H. Schune,⁷ R. Schwemmer,³⁸ B. Sciascia,¹⁸ A. Sciubba,^{25,s} A. Semennikov,³¹ I. Sepp,⁵³ N. Serra,⁴⁰ J. Serrano,⁶ L. Sestini,²² P. Seyfert,¹¹ M. Shapkin,³⁵ I. Shapoval,^{16,43,b} Y. Shcheglov,³⁰ T. Shears,⁵² L. Shekhtman,³⁴ V. Shevchenko,⁶⁴ A. Shires,⁹ R. Silva Coutinho,⁴⁸ G. Simi,²² M. Sirendi,⁴⁷ N. Skidmore,⁴⁶ I. Skillicorn,⁵¹ T. Skwarnicki,⁵⁹ N. A. Smith,⁵² E. Smith,^{55,49} E. Smith,⁵³ J. Smith,⁴⁷ M. Smith,⁵⁴ H. Snoek,⁴¹ M. D. Sokoloff,⁵⁷ F. J. P. Soler,⁵¹ F. Soomro,³⁹ D. Souza,⁴⁶ B. Souza De Paula,² B. Spaan,⁹ P. Spradlin,⁵¹ S. Sridharan,³⁸ F. Stagni,³⁸ M. Stahl,¹¹ S. Stahl,¹¹ O. Steinkamp,⁴⁰ O. Stenyakin,³⁵ F. Sterpka,⁵⁹ S. Stevenson,⁵⁵ S. Stoica,²⁹ S. Stone,⁵⁹ B. Storaci,⁴⁰ S. Stracka,^{23,j} M. Straticiu,²⁹ U. Straumann,⁴⁰ R. Stroili,²² L. Sun,⁵⁷ W. Sutcliffe,⁵³ K. Swientek,²⁷ S. Swientek,⁹ V. Syropoulos,⁴² M. Szczekowski,²⁸ P. Szczypka,^{39,38} T. Szumlak,²⁷ S. T'Jampens,⁴ M. Teklishyn,⁷ G. Tellarini,^{16,b} F. Teubert,³⁸ C. Thomas,⁵⁵ E. Thomas,³⁸ J. van Tilburg,⁴¹ V. Tisserand,⁴ M. Tobin,³⁹ J. Todd,⁵⁷ S. Tolk,⁴² L. Tomassetti,^{16,b} D. Tonelli,³⁸ S. Topp-Joergensen,⁵⁵ N. Torr,⁵⁵ E. Tournefier,⁴ S. Tourneur,³⁹ M. T. Tran,³⁹ M. Tresch,⁴⁰ A. Trisovic,³⁸ A. Tsaregorodtsev,⁶ P. Tsopelas,⁴¹ N. Tuning,⁴¹ M. Ubeda Garcia,³⁸ A. Ukjeja,²⁸ A. Ustyuzhanin,⁶⁴ U. Uwer,¹¹ C. Vacca,¹⁵ V. Vagnoni,¹⁴ G. Valenti,¹⁴ A. Vallier,⁷ R. Vazquez Gomez,¹⁸ P. Vazquez Regueiro,³⁷ C. Vázquez Sierra,³⁷ S. Vecchi,¹⁶ J. J. Velthuis,⁴⁶ M. Veltri,^{17,u} G. Veneziano,³⁹ M. Vesterinen,¹¹ JVV B Viana Barbosa,³⁸ B. Viaud,⁷ D. Vieira,² M. Vieites Diaz,³⁷ X. Vilasis-Cardona,^{36,f} A. Vollhardt,⁴⁰ D. Volyansky,¹⁰ D. Voong,⁴⁶ A. Vorobyev,³⁰ V. Vorobyev,³⁴ C. Voß,⁶³ J. A. de Vries,⁴¹ R. Waldi,⁶³ C. Wallace,⁴⁸ R. Wallace,¹² J. Walsh,²³ S. Wandernoth,¹¹ J. Wang,⁵⁹ D. R. Ward,⁴⁷ N. K. Watson,⁴⁵ D. Websdale,⁵³ M. Whitehead,⁴⁸ D. Wiedner,¹¹ G. Wilkinson,^{55,38} M. Wilkinson,⁵⁹ M. P. Williams,⁴⁵ M. Williams,⁵⁶ H. W. Wilschut,⁶⁶ F. F. Wilson,⁴⁹ J. Wimberley,⁵⁸ J. Wishahi,⁹ W. Wislicki,²⁸ M. Witek,²⁶ G. Wormser,⁷ S. A. Wotton,⁴⁷ S. Wright,⁴⁷ K. Wyllie,³⁸ Y. Xie,⁶¹ Z. Xing,⁵⁹ Z. Xu,³⁹ Z. Yang,³ X. Yuan,³ O. Yushchenko,³⁵ M. Zangoli,¹⁴ M. Zavertyaev,^{10,v} L. Zhang,³ W. C. Zhang,¹² Y. Zhang,³ A. Zhelezov,¹¹ A. Zhokhov,³¹ and L. Zhong³

(LHCb Collaboration)

¹Centro Brasileiro de Pesquisas Físicas (CBPF), Rio de Janeiro, Brazil²Universidade Federal do Rio de Janeiro (UFRJ), Rio de Janeiro, Brazil³Center for High Energy Physics, Tsinghua University, Beijing, China⁴LAPP, Université de Savoie, CNRS/IN2P3, Annecy-Le-Vieux, France⁵Clermont Université, Université Blaise Pascal, CNRS/IN2P3, LPC, Clermont-Ferrand, France

- ⁶CPPM, Aix-Marseille Université, CNRS/IN2P3, Marseille, France
- ⁷LAL, Université Paris-Sud, CNRS/IN2P3, Orsay, France
- ⁸LPNHE, Université Pierre et Marie Curie, Université Paris Diderot, CNRS/IN2P3, Paris, France
- ⁹Fakultät Physik, Technische Universität Dortmund, Dortmund, Germany
- ¹⁰Max-Planck-Institut für Kernphysik (MPIK), Heidelberg, Germany
- ¹¹Physikalisches Institut, Ruprecht-Karls-Universität Heidelberg, Heidelberg, Germany
- ¹²School of Physics, University College Dublin, Dublin, Ireland
- ¹³Sezione INFN di Bari, Bari, Italy
- ¹⁴Sezione INFN di Bologna, Bologna, Italy
- ¹⁵Sezione INFN di Cagliari, Cagliari, Italy
- ¹⁶Sezione INFN di Ferrara, Ferrara, Italy
- ¹⁷Sezione INFN di Firenze, Firenze, Italy
- ¹⁸Laboratori Nazionali dell'INFN di Frascati, Frascati, Italy
- ¹⁹Sezione INFN di Genova, Genova, Italy
- ²⁰Sezione INFN di Milano Bicocca, Milano, Italy
- ²¹Sezione INFN di Milano, Milano, Italy
- ²²Sezione INFN di Padova, Padova, Italy
- ²³Sezione INFN di Pisa, Pisa, Italy
- ²⁴Sezione INFN di Roma Tor Vergata, Roma, Italy
- ²⁵Sezione INFN di Roma La Sapienza, Roma, Italy
- ²⁶Henryk Niewodniczanski Institute of Nuclear Physics Polish Academy of Sciences, Kraków, Poland
- ²⁷AGH - University of Science and Technology, Faculty of Physics and Applied Computer Science, Kraków, Poland
- ²⁸National Center for Nuclear Research (NCBJ), Warsaw, Poland
- ²⁹Horia Hulubei National Institute of Physics and Nuclear Engineering, Bucharest-Magurele, Romania
- ³⁰Petersburg Nuclear Physics Institute (PNPI), Gatchina, Russia
- ³¹Institute of Theoretical and Experimental Physics (ITEP), Moscow, Russia
- ³²Institute of Nuclear Physics, Moscow State University (SINP MSU), Moscow, Russia
- ³³Institute for Nuclear Research of the Russian Academy of Sciences (INR RAN), Moscow, Russia
- ³⁴Budker Institute of Nuclear Physics (SB RAS) and Novosibirsk State University, Novosibirsk, Russia
- ³⁵Institute for High Energy Physics (IHEP), Protvino, Russia
- ³⁶Universitat de Barcelona, Barcelona, Spain
- ³⁷Universidad de Santiago de Compostela, Santiago de Compostela, Spain
- ³⁸European Organization for Nuclear Research (CERN), Geneva, Switzerland
- ³⁹Ecole Polytechnique Fédérale de Lausanne (EPFL), Lausanne, Switzerland
- ⁴⁰Physik-Institut, Universität Zürich, Zürich, Switzerland
- ⁴¹Nikhef National Institute for Subatomic Physics, Amsterdam, The Netherlands
- ⁴²Nikhef National Institute for Subatomic Physics and VU University Amsterdam, Amsterdam, The Netherlands
- ⁴³NSC Kharkiv Institute of Physics and Technology (NSC KIPT), Kharkiv, Ukraine
- ⁴⁴Institute for Nuclear Research of the National Academy of Sciences (KINR), Kyiv, Ukraine
- ⁴⁵University of Birmingham, Birmingham, United Kingdom
- ⁴⁶H H Wills Physics Laboratory, University of Bristol, Bristol, United Kingdom
- ⁴⁷Cavendish Laboratory, University of Cambridge, Cambridge, United Kingdom
- ⁴⁸Department of Physics, University of Warwick, Coventry, United Kingdom
- ⁴⁹STFC Rutherford Appleton Laboratory, Didcot, United Kingdom
- ⁵⁰School of Physics and Astronomy, University of Edinburgh, Edinburgh, United Kingdom
- ⁵¹School of Physics and Astronomy, University of Glasgow, Glasgow, United Kingdom
- ⁵²Oliver Lodge Laboratory, University of Liverpool, Liverpool, United Kingdom
- ⁵³Imperial College London, London, United Kingdom
- ⁵⁴School of Physics and Astronomy, University of Manchester, Manchester, United Kingdom
- ⁵⁵Department of Physics, University of Oxford, Oxford, United Kingdom
- ⁵⁶Massachusetts Institute of Technology, Cambridge, Massachusetts, USA
- ⁵⁷University of Cincinnati, Cincinnati 45221 Ohio, USA
- ⁵⁸University of Maryland, College Park 20742 Maryland, USA
- ⁵⁹Syracuse University, Syracuse 13244 New York, USA
- ⁶⁰Pontificia Universidade Católica do Rio de Janeiro (PUC-Rio), Rio de Janeiro, Brazil
(associated with Institution Universidade Federal do Rio de Janeiro (UFRJ), Rio de Janeiro, Brazil)
- ⁶¹Institute of Particle Physics, Central China Normal University, Wuhan, Hubei, China
(associated with Institution Center for High Energy Physics, Tsinghua University, Beijing, China)
- ⁶²Departamento de Física, Universidad Nacional de Colombia, Bogota, Colombia (associated with Institution LPNHE, Université Pierre et Marie Curie, Université Paris Diderot, CNRS/IN2P3, Paris, France)

⁶³*Institut für Physik, Universität Rostock, Rostock, Germany (associated with Institution Physikalisches Institut, Ruprecht-Karls-Universität Heidelberg, Heidelberg, Germany)*

⁶⁴*National Research Centre Kurchatov Institute, Moscow, Russia (associated with Institution Institute of Theoretical and Experimental Physics (ITEP), Moscow, Russia)*

⁶⁵*Instituto de Fisica Corpuscular (IFIC), Universitat de Valencia-CSIC, Valencia, Spain (associated with Institution Universitat de Barcelona, Barcelona, Spain)*

⁶⁶*Van Swinderen Institute, University of Groningen, Groningen, The Netherlands (associated with Institution Nikhef National Institute for Subatomic Physics, Amsterdam, The Netherlands)*

⁶⁷*Celal Bayar University, Manisa, Turkey (associated with Institution European Organization for Nuclear Research (CERN), Geneva, Switzerland)*

^aAlso at Università di Firenze, Firenze, Italy.

^bAlso at Università di Ferrara, Ferrara, Italy.

^cAlso at Università della Basilicata, Potenza, Italy.

^dAlso at Università di Modena e Reggio Emilia, Modena, Italy.

^eAlso at Università di Milano Bicocca, Milano, Italy.

^fAlso at LIFAELS, La Salle, Universitat Ramon Llull, Barcelona, Spain.

^gAlso at Università di Bologna, Bologna, Italy.

^hAlso at Università di Roma Tor Vergata, Roma, Italy.

ⁱAlso at Università di Genova, Genova, Italy.

^jAlso at Scuola Normale Superiore, Pisa, Italy.

^kAlso at Politecnico di Milano, Milano, Italy.

^lAlso at Universidade Federal do Triângulo Mineiro (UFTM), Uberaba-MG, Brazil.

^mAlso at AGH - University of Science and Technology, Faculty of Computer Science, Electronics and Telecommunications, Kraków, Poland.

ⁿAlso at Università di Padova, Padova, Italy.

^oAlso at Università di Cagliari, Cagliari, Italy.

^pAlso at Hanoi University of Science, Hanoi, Viet Nam.

^qAlso at Università di Bari, Bari, Italy.

^rAlso at Università degli Studi di Milano, Milano, Italy.

^sAlso at Università di Roma La Sapienza, Roma, Italy.

^tAlso at Università di Pisa, Pisa, Italy.

^uAlso at Università di Urbino, Urbino, Italy.

^vAlso at P.N. Lebedev Physical Institute, Russian Academy of Science (LPI RAS), Moscow, Russia.